Nanoscale Res Lett (2010) 5:761–768
DOI 10.1007/s11671-010-9554-9

NANO EXPRESS

Structure and Luminescence Properties of Eu^{3+}-Doped Cubic Mesoporous Silica Thin Films

Qingshan Lu · Zhongying Wang · Peiyu Wang · Jiangong Li

Received: 20 November 2009 / Accepted: 28 January 2010 / Published online: 11 February 2010

Abstract Eu^{3+} ions-doped cubic mesoporous silica thin films with a thickness of about 205 nm were prepared on silicon and glass substrates using triblock copolymer as a structure-directing agent using sol–gel spin-coating and calcination processes. X-ray diffraction and transmission electron microscopy analysis show that the mesoporous silica thin films have a highly ordered body-centered cubic mesoporous structure. High Eu^{3+} ion loading and high temperature calcination do not destroy the ordered cubic mesoporous structure of the mesoporous silica thin films. Photoluminescence spectra show two characteristic emission peaks corresponding to the transitions of $^5D_0$-$^7F_1$ and $^5D_0$-$^7F_2$ of Eu^{3+} ions located in low symmetry sites in mesoporous silica thin films. With the Eu/Si molar ratio increasing to 3.41%, the luminescence intensity of the Eu^{3+} ions-doped mesoporous silica thin films increases linearly with increasing Eu^{3+} concentration.

Keywords Luminescence · Eu^{3+} doping · Cubic mesoporous · Thin film · Sol–gel

Introduction

Preparation of mesoporous silica thin films (MTFs) by evaporation-induced self-assembly took its origins from the pioneer work by Mobil on surfactant-templated materials [1]. The study on MTFs was reported by Ozin's and Brinker's groups [2, 3]. Since then, a variety of mesoporous thin films have attracted a great deal of attention because of their controllable structures and compositions as well as their potential applications as catalyst supports [3], optical devices [4, 5], sensors [6], low-*k*-dielectrics [7], and membranes [8]. MTFs have large surface areas, ordered porous structures, and uniform pore size distributions and can serve as excellent hosts for homogeneous distribution of functional guest species without aggregation. Up to date, many studies were focused on fabricating the hybrid materials with improved performance by introducing functional guest species into the pores of mesoporous silica thin films [9–11]. It was reported that well-ordered mesoporous titania thin films can act as a host matrix for luminescence rare earth ions [12–14], and Eu could be doped up to 8.0% Eu/Ti molar ratio without luminescence quenching occurring [14]. Cubic mesoporous titania thin film doped with Cr^{3+} exhibited superior visible light photocatalytic activity [15].

The special luminescence properties of lanthanide ion-doped nanomaterials with various inorganic hosts have found applications in many fields including displays, optical telecommunications, lasers, infrared-to-visible-light up-conversion, and optoelectronic devices. Rare earth ions-doped glasses have been extensively studied as potential materials for various optical devices. Luminescence properties of europium ions doped in oxide glasses using a sol–gel process have been investigated during the last decade [16–18] because of their usefulness in various applications due to its sharp, near-monochromatic emission lines. Furthermore, the Eu^{3+} ion is a sensitive optical probe for the dopant site environment or symmetry because of its particular luminescence spectrum [19]. Currently, the luminescence efficiency of Eu^{3+} ions in sol–gel host materials is limited due to concentration fluorescence quenching originated from the aggregation and cluster formation of

Q. Lu · Z. Wang · P. Wang · J. Li (✉)
Institute of Materials Science and Engineering and MOE Laboratory for Magnetism and Magnetic Materials, Lanzhou University, 730000 Lanzhou, China
e-mail: lijg@lzu.edu.cn

Eu^{3+} ions and due to hydroxyl quenching resulted from the presence of residual water, solvents, and hydroxyl groups. These two problems must be solved to achieve practical optical devices based on Eu^{3+} ions-doped sol–gel glasses. The solubility of Eu in silica glass is very limited. The high Eu^{3+} concentration results in fluorescence quenching. Practically, fluorescence quenching is evident for Eu content higher than 1% (molar ratio) in silica glass [20]. In comparison with bulk silica, ordered mesoporous silica provides a unique structure; the luminescence of Eu^{3+} ions can be used to probe the chemical environment of the Eu^{3+} ions. In addition, ordered mesoporous silica thin films with large surface areas may load relatively high content of Eu^{3+} ions without the aggregation of Eu^{3+} ions, because they can provide enough non-network oxygen species from amorphous silica walls and inner surface areas to coordinate and charge compensate the Eu^{3+} ions [16]. Furthermore, the mesoporous silica thin films have a low cost, good thermal, and moisture stability. Therefore, the development of mesoporous silica thin film as an inorganic host matrix for europium ions is of importance.

In the present work, we prepared Eu^{3+} ions-doped cubic mesoporous silica thin films and studied their structure and luminescence properties. The results reveal that the thin films keep well-ordered mesoporous structures, even with high Eu^{3+} ion loading and calcined at high temperature. Photoluminescence spectra show two characteristic emission peaks of Eu^{3+} ions as emission centers. The Eu^{3+} content of Eu/Si molar ratio up to 3.41% could be doped in mesoporous silica thin film without fluorescence quenching occurring. Our study presents an interesting optical application of an all-inorganic mesoporous material.

Experiment Section

Preparation

In a typical synthesis, Eu^{3+} ions-doped ordered cubic mesoporous silica thin films were coated on glass substrates and crystal silicon wafers by spin-coating via evaporation-induced self-assembly [21]. The precursor for the coating sol solution was prepared in the following procedure. The polymeric silica sol was prepared by stirring a mixture of 2.08 g tetraethoxy silane (TEOS), 6 g ethanol (EtOH), and 1.8 g 0.7 M dilute hydrochloric acid (HCl) at room temperature for 1 h. Then, the silica sol was added into a solution containing 8 g ethanol and 0.67 g triblock copolymer $HO(CH_2CH_2O)_{106}[CH_2CH(CH_3)O]_{70}(CH_2CH_2O)_{106}H$ (abbreviated as $EO_{106}PO_{70}EO_{106}$, Pluronic F-127, Aldrich). After stirring a few minutes, an amount of europium nitrate $[Eu(NO_3)_3 \cdot 6H_2O]$ was added to the mixed solution. Finally, a clear solution with the molar ratio of $TEOS:F127:H_2O:HCl:EtOH:Eu(NO_3)_3 = 1:0.005:10:0.13:30:x$ (x ranging from 0.005 to 0.06) was obtained after 2-h continuous stirring at room temperature. Then, the coating solution was spin-coated on cleaned glass substrates or silicon wafers rotating at a speed of 2,000 rpm for 10 s. The films were stored for 48 h at room temperature and then calcined at different temperatures for 4 h in air at a heating rate of 1°C/min to obtain Eu^{3+} ions-doped mesoporous silica thin films.

Characterizations

The content of Eu in the Eu^{3+}-doped mesoporous silica thin film was analyzed using an IRIS Advantage inductively coupled plasma atomic emission spectrometry (ICP-AES). Differential thermal analysis (DTA) and thermogravimetry (TG) measurements were taken on a Pyris Diamond thermoanalyzer in air at a heating rate of 20°C/min. Low-angle and wide-angle X-ray diffraction (XRD) measurements were taken on a Rigaku D/Max-2400 X-ray diffractometer using Cu K_α radiation in θ-2θ scan mode. High-resolution transmission electron microscope (HRTEM) analysis and energy dispersive spectroscopy (EDS) measurements were taken using a Philips Tecnai F30 FEG-TEM electron microscope operated at 300 kV. The specimens for the TEM observations were prepared by removing the films from the substrates using a blade and suspending them in ethanol. This suspension solution was then dropped on a holey carbon film supported by a copper grid. Cross-section scanning electron microscope (SEM) observations of the films were conducted on a Hitachi S4800 field emission SEM at an accelerating voltage of 5 kV. The attenuated total reflection Fourier transform infrared (ATR-FTIR) spectra of the Eu^{3+}-doped cubic mesoporous silica films deposited on single crystal silicon wafers were recorded on a Nicolet Nexus 670 FT-IR spectrometer using 4 cm^{-1} resolution and 60 scans. Room temperature photoluminescence spectra of the Eu^{3+}-doped cubic mesoporous silica films deposited on single crystal silicon wafers were recorded on a FLS-920T fluorescence spectrophotometer using Xe 900 (450-W xenon arc lamp) as the light source using an excitation wavelength of 246 nm. The slit was 0.2 nm for the excitation spectra and 2.0 nm for the emission spectra. The step was 0.5 nm, and the dwell time was 0.2 s.

Results and Discussion

Structure of Eu^{3+} Ions-Doped Mesoporous Silica Thin Films

Table 1 lists the ICP-AES analysis results of Eu/Si molar ratio for the Eu^{3+}-doped mesoporous silica thin films. For each sample, the Eu/Si molar ratio determined by the

Table 1 The Eu/Si molar ratios of the Eu^{3+}-doped mesoporous silica thin films estimated from the solution compositions and determined by the ICP-AES analysis

Sample	Eu/Si molar ratios estimated from the solution compositions (%)	Eu/Si molar ratios determined by the ICP-AES analysis (%)
1	0.5	0.44
2	1.0	0.87
3	3.0	2.57
4	4.0	3.41
5	6.0	5.24

ICP-AES analysis is lower than that estimated from the solution compositions. In the subsequent discussion, the Eu/Si molar ratios determined by the ICP-AES analysis are used.

The structural evolution of Eu^{3+}-doped mesoporous silica thin film related to the decomposition of surfactant F127 during heat treatment is studied. The spontaneous organization of silica–surfactant mesophases involving silica frameworks and surfactant regions is formed by sol–gel and spin-coating processes. During the calcination treatment, the surfactant F127 decomposes, and the contraction of the mesoporous structure occurs. The DTA and TG curves for the as-spin-coated Eu^{3+}-doped mesoporous silica thin film with an Eu/Si molar ratio of 0.44% are shown in Fig. 1. A small weight loss from 50 to 120°C is due to the loss of physically adsorbed water. A large weight loss from 160 to 500°C accompanied by two exothermic peaks centered at about 236 and 369°C is attributed to the decomposition and combustion of surfactant F127 [22]. The surfactant F127 can be completely removed above 500°C.

Figure 2 shows the TEM micrographs of the Eu^{3+} ions-doped mesoporous silica thin films with an Eu^{3+}/Si molar ratio of 2.57% calcined at 400°C for 4 h. Figure 2a exhibits

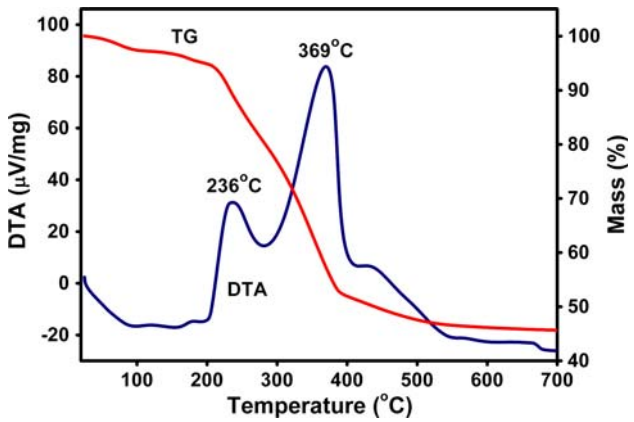

Fig. 1 The TG-DTA curves of the spin-coated Eu^{3+} ions-doped mesoporous silica thin film with an Eu/Si molar ratio of 0.44%

ordered pore arrangement with the configuration of four coordination pores. Figure 2b displays ordered pore structure with the configuration of six coordination pores. The fast Fourier transform images with the fourfold symmetry and the sixfold symmetry in Fig. 2 suggest that the Eu^{3+} ions-doped mesoporous silica thin film formed with template $EO_{106}PO_{70}EO_{106}$ has a highly ordered body-centered cubic structure with the *Im*3 *m* space group. This structure seems to be the same as that reported for the body-centered cubic (*Im*3 *m* space group) mesoporous silica and titania thin films with the (100) planes parallel to the substrate [23, 24]. The average diameter of the ordered pores in the body-centered cubic structure was estimated to be 3.8 nm according to the TEM observations. No guest particles such as europium oxide particles could be observed in the mesoporous thin films by TEM. The cross-sectional SEM image in Fig. 3 reveals that the Eu^{3+} ions-doped mesoporous silica thin film is continuous, smooth, and dense on the silicon wafer and has the thickness of about 205 nm.

Figure 4 shows the low-angle XRD patterns of the Eu^{3+} ions-doped mesoporous silica thin films with an Eu/Si molar ratio of 2.57% calcined at different temperatures for 4 h. As shown in Fig. 4a, all of the calcined film samples have the intense main peaks; and Fig. 4b shows the relative weak peaks attributed to the second-order reflection. The main peak and the relative weak peak can be indexed as (200) and (400) reflections of a body-centered cubic mesophase, respectively, indicating that the Eu^{3+} ions-doped mesoporous silica thin films have an ordered mesoporous structure [24]. This is in good agreement with the TEM analysis results. With calcining temperature increasing from 100 to 600°C, the diffraction peaks shift clearly to high angles, and the d_{200} interplanar spacing in the out-of-plane direction of the films decreases from 10.6 to 5.9 nm. This should be due to the contraction of the mesoporous structure often observed after removal of the organic template and further condensation of the silica framework during the calcination treatment [25]. It is noticed that the Eu^{3+} ions-doped mesoporous silica thin films can be calcined at temperature up to 600°C and do not loss the mesostructural ordering. This indicates that the Eu^{3+} ions-doped cubic mesoporous silica thin films have a high thermal stability.

The wide-angle XRD patterns of the Eu^{3+} ions-doped mesoporous silica thin films with an Eu/Si molar ratio of 2.57% calcined at different temperatures in Fig. 5 show only the diffuse peaks of the non-crystalline silica. There are no detectable diffraction peaks of the Eu_2O_3 crystalline phase, even for the film calcined at 600°C. This implies that the Eu^{3+} ions are well doped in the mesoporous silica thin films without any Eu_2O_3 crystalline phase formed. There are a lot of non-network oxygen species on the non-crystalline silica walls and large inner surface areas in the

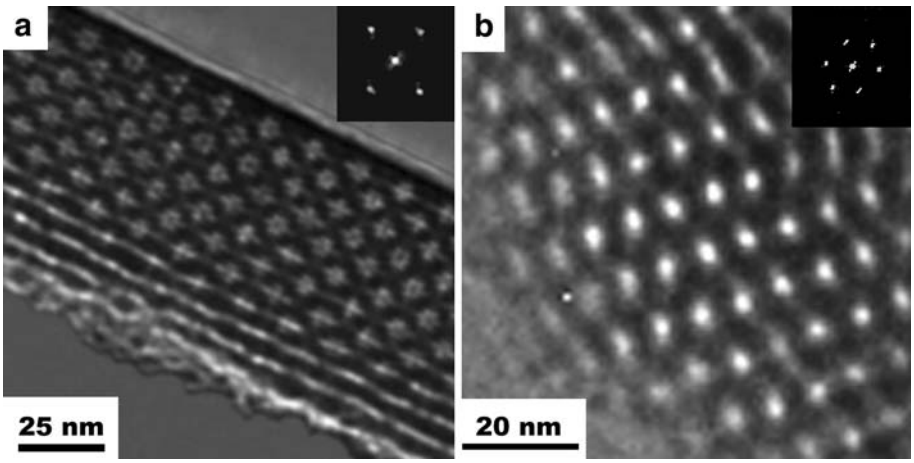

Fig. 2 The TEM micrographs of the Eu^{3+} ions-doped mesoporous silica thin film with an Eu/Si molar ratio of 2.57% calcined at 400°C for 4 h along the [100] direction (**a**) and the [111] direction (**b**) of the body-centered cubic (*Im3 m*) mesostructure. The corresponding Fourier-transform patterns of the images are shown in the *insets*

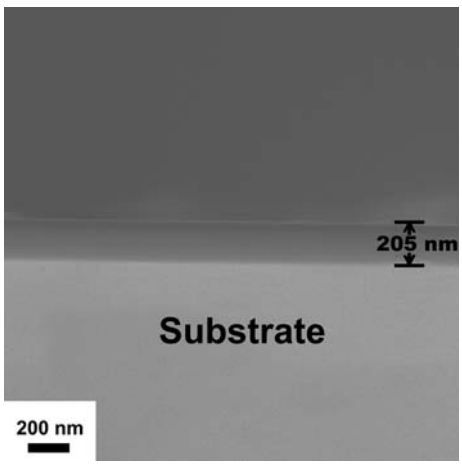

Fig. 3 The cross-sectional SEM micrograph of the Eu^{3+} ions-doped mesoporous silica thin film with an Eu/Si molar ratio of 2.57% calcined at 500°C for 4 h on a silicon wafer

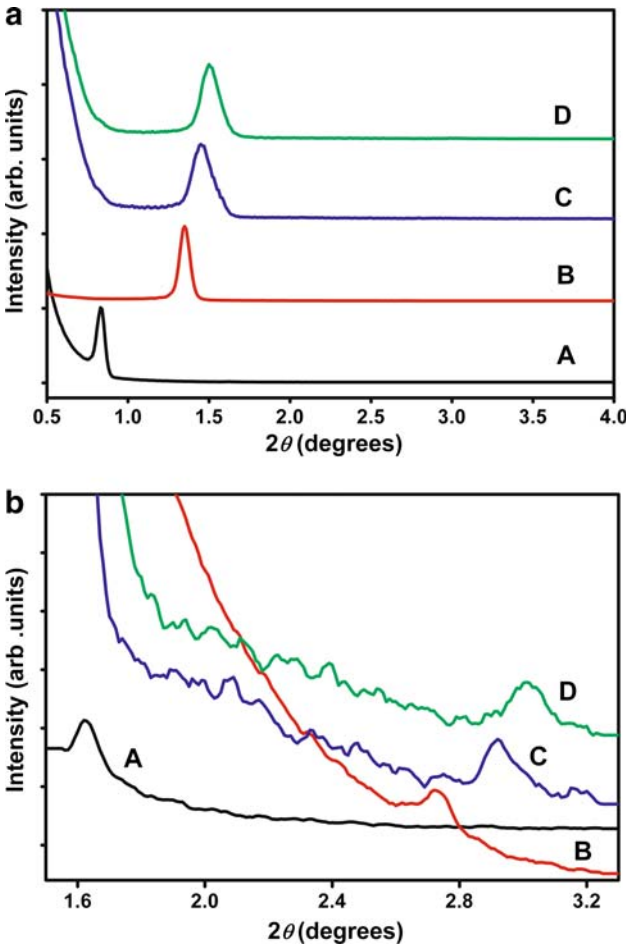

Fig. 4 The low-angle XRD patterns of the Eu^{3+} ions-doped mesoporous silica thin films with an Eu/Si molar ratio of 2.57% calcined at 100°C (*curve A*), 400°C (*curve B*), 500°C (*curve C*), and 600°C (*curve D*) for 4 h (Fig. 4a) and corresponding second-order reflections (Fig. 4b)

mesoporous silica thin film [16], in comparison with the pure non-crystalline silica without nanoscale pores. The coordination and charge compensation of the Eu^{3+} ions with non-network oxygens occur during sol–gel and calcination process.

To further analyze the effect of the Eu^{3+} ions doping concentration and calcination temperature on the mesoporous structure and phase structure of the Eu^{3+} ions-doped mesoporous silica thin films, the film sample with a high Eu/Si molar ratio of 5.24% annealed at a high temperature of 600°C for 4 h was analyzed using XRD. As shown in Fig. 6, the low-angle XRD pattern of this sample shows an intense main peak with a weak secondary reflection, confirming the ordered mesoporous structure which is same as that of the Eu^{3+} ions-doped mesoporous silica thin films with an Eu/Si molar ratio of 2.57% calcined at 600°C. This suggests that mesoporous silica thin film used as host matrix can load a large amount of guest species without losing ordered mesoporous structure. The wide-angle XRD pattern of this sample shows only an intense peak at $2\theta = 69°$ belonging to the (100) diffraction of the single crystal Si substrate. No diffraction peaks from

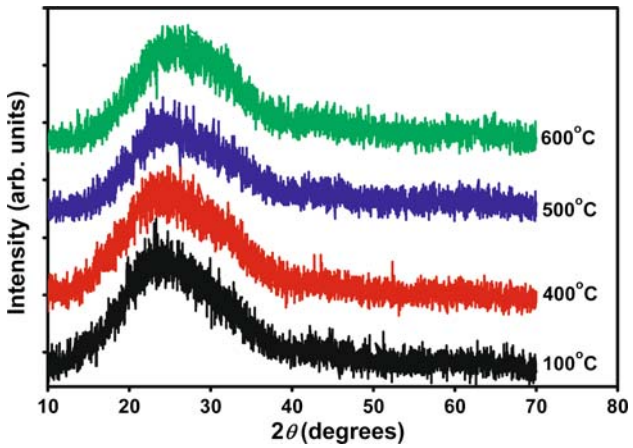

Fig. 5 The wide-angle XRD patterns of the Eu^{3+} ions-doped mesoporous silica thin films with an Eu/Si molar ratio of 2.57% calcined at different temperatures

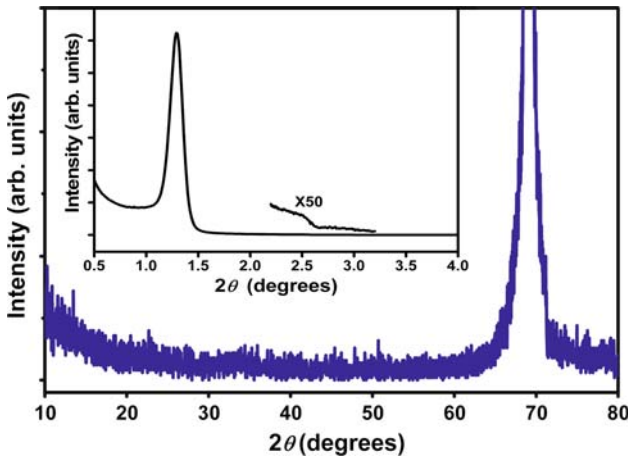

Fig. 6 The wide-angle XRD pattern and low-angle XRD pattern (*inset*) of the Eu^{3+} ions-doped mesoporous silica thin film with an Eu/Si molar ratio of 5.24% calcined at 600°C for 4 h

the crystalline europium oxides is present in the XRD pattern, indicating that no crystalline phases of the europium oxides form in the sample.

Figure 7 shows the FTIR spectra of the Eu^{3+} ion-doped cubic mesoporous silica thin film with an Eu/Si molar ratio of 2.57%. Curve A and curve B in Fig. 7 represent the FTIR spectra of the spin-coated thin film and the thin film calcined at 600°C, respectively. The bands in the range from 700 to 1,200 cm^{-1} in curve A (Fig. 7) can be attributed to the Si–O–Si and the silanol Si–OH vibration [26]. For example, the bands at around 797 and 1,042 cm^{-1} are originated from the Si–O–Si asymmetric stretching vibration and Si–O–Si symmetric stretching vibration, respectively. The band at around 947 cm^{-1} is assigned to the silanol Si–OH band stretching vibration. Several infrared adsorption bands at around 1,347, 1,446, 2,874, and 2,913 cm^{-1} can be related to the C–H stretching and

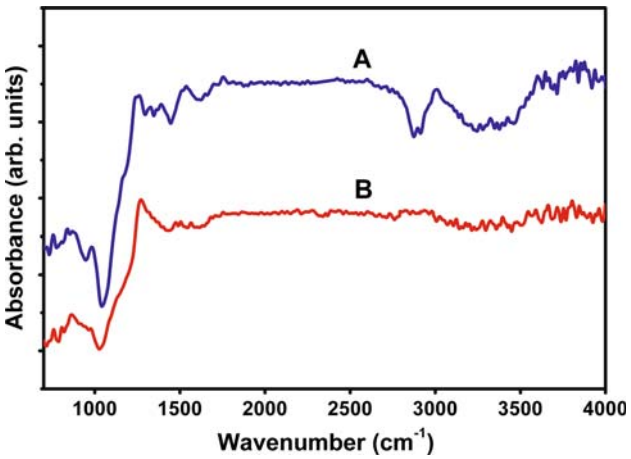

Fig. 7 FTIR spectra of the Eu^{3+} ion-doped cubic mesoporous silica thin films with an Eu/Si molar ratio of 2.57% spin-coated (*curve A*) and calcined at 600°C for 4 h (*curve B*)

bending vibrations of the triblock copolymer F-127 [27]. Furthermore, a broad band centered at around 3,380 cm^{-1} is attributed to the O–H stretching vibration mode of the adsorbed H_2O molecules, and the band at 1,621 cm^{-1} is assigned to the bending vibration mode of the adsorbed H_2O [28]. Comparing the calcined film with the spin-coated film, the intensity of the Si–OH bending band at around 947 cm^{-1} is much weaker than that of the spin-coated film sample, implying the reduction in the silanol number on the pore wall surface. The disappearance of the bands for the C–H stretching and bending vibrations indicates the efficient removal of the organic template F-127 from the film by calcination. In addition, a strong decrease in the infrared adsorption bands at around 1,621 and 3,380 cm^{-1} is indicative of the decrease in the adsorbed H_2O in Eu^{3+} ion-doped cubic mesoporous silica thin film after calcination treatment.

To confirm the presence of Eu in the Eu^{3+} ions-doped mesoporous silica thin films, the EDS analysis was carried out in the TEM observations. The EDS spectrum of the Eu^{3+} ions-doped mesoporous silica thin film with an Eu/Si molar ratio of 2.57% calcined at 600°C for 4 h is shown in Fig. 8. The elements C and Cu come from the supporting carbon film and the copper grid, respectively. The Eu peaks confirm the presence of Eu^{3+} ions in the Eu^{3+} ions-doped cubic mesoporous silica thin films.

A schematic drawing showing the structure formation process of the Eu^{3+} ions-doped mesoporous silica thin film is shown in Fig. 9. A homogeneous sol solution involving surfactant F127, silica precursor (inorganic entities), and europium ions is formed by sol–gel method. During the spin-coating process, the phase segregation and the self-assembly will result in spontaneous organization of silica–surfactant mesophases which involve inorganic frameworks and surfactant regions. The Eu^{3+} ions are

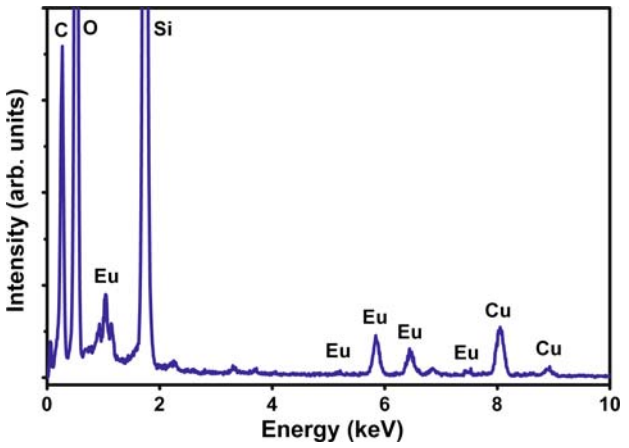

Fig. 8 The EDS spectrum of the Eu^{3+} ions-doped mesoporous silica thin film with an Eu/Si molar ratio of 2.57% calcined at 600°C for 4 h. The elemental C and Cu peaks are from the supporting carbon film and the copper grid, respectively

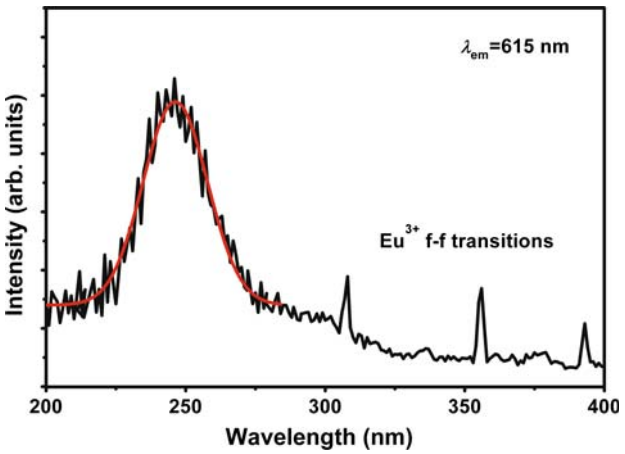

Fig. 10 The excitation spectrum of the Eu^{3+} ions-doped mesoporous silica thin film with an Eu/Si molar ratio of 3.41% calcined at 600°C for 4 h measured using a monitor wavelength of 615 nm

incorporated into non-crystalline silica frameworks as in the Eu-doped non-crystalline regions of mesoporous TiO_2 particles [29]. During calcination, the surfactant F127 decomposes, and some Eu^{3+} ions would diffuse from the non-crystalline regions to the large surface areas to coordinate and to charge compensate non-network oxygen species [30]. The Eu^{3+} ions are mainly doped in the frameworks of mesoporous silica. In addition, there are some Eu^{3+} ions on the large surface of the frameworks.

Luminescence Properties

The excitation spectrum of the Eu^{3+} ions-doped mesoporous silica thin film with an Eu/Si molar ratio of 3.41% calcined at 600°C for 4 h was measured using a monitor wavelength of 615 nm and is shown in Fig. 10. This excitation spectrum consists of a broad band and several narrow peaks. The broad band centers at around 246 nm; and the narrow peaks locate at around 308, 356, and 393 nm. The broad band centered at around 246 nm is due to the charge-transfer band (CTB) of Eu^{3+}–O^{2-}. The peaks at around 308, 356, and 393 nm are attributed to f–f transitions within the Eu^{3+} $4f^6$ electron configuration. The emission peaks assigned to the f–f transitions of the Eu^{3+} ion are narrow due to the shielding of the 4f orbitals by the outer $5s^2$ and $5p^6$ orbitals [31]. In the present work, the f–f transitions are similar to those observed for europium ion-doped other oxides, fluorophosphates, and fluorogallate glasses. The center of the Eu^{3+}–O^{2-} CTB is located at about 246 nm determined by Gaussian fitting; and this band shifts slightly to short-wavelength in comparison with that in some of oxides [32] and zeolite-A [33]. This is because the charge transition process much depends on the bonding environment and the activator characteristic in RE-doped compounds. Accordingly, we attribute the broad, intense band with a maximum at 246 nm in the excitation spectrum to the charge transfer state from the silica framework oxygen ions to europium ions. The Eu^{3+}–O^{2-} CTB is much similar with the 253 nm band for $SiO_2@Y_2SiO_5:Eu^{3+}$ [34]. The appearance of the charge transfer state in the excitation spectrum indicates the coordination of the europium ions with the oxygen ions in the silica.

Room temperature photoluminescence spectra of the Eu^{3+} ions-doped mesoporous silica thin films with an Eu/Si molar ratio of 2.57% upon excitation of 246 nm are shown in Fig. 11. The Eu^{3+} ions-doped mesoporous silica thin films calcined at different temperatures ranging from 100 to 600°C yield similar emission spectra. All the observed peaks correspond to the transitions from the metastable orbital singlet state $^5D_0$ level to the spin–orbit states of ^7F_J ($J = 1, 2$) level of Eu^{3+} ions. The transitions from the $^5D_0$ to $^7F_1$ (bands between 586 and 597 nm) and

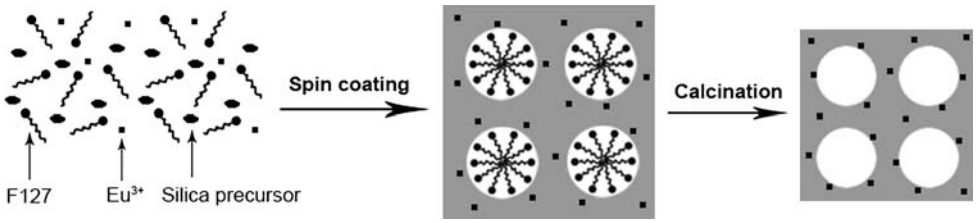

Fig. 9 A schematic drawing showing the structure formation process of the Eu^{3+} ions-doped mesoporous silica thin film

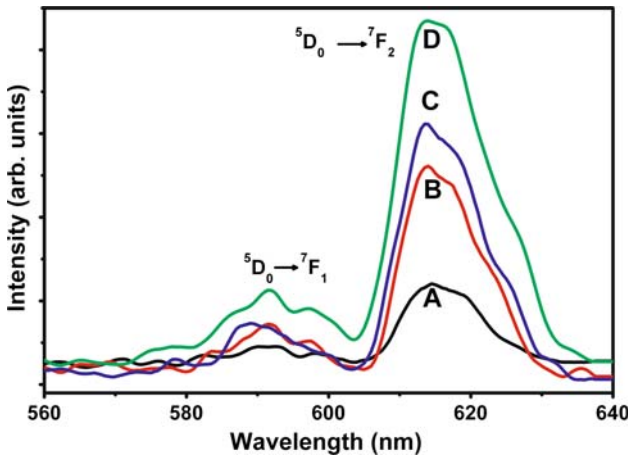

Fig. 11 The luminescence spectra of the Eu^{3+} ions-doped mesoporous silica thin films with an Eu/Si molar ratio of 2.57% calcined at 100°C (*curve A*), 400°C (*curve B*), 500°C (*curve C*), and 600°C (*curve D*) for 4 h

$^7F_2$ (bands between 612 and 617 nm) are the characteristic emissions of the Eu^{3+} ions under excitation [35]. In all cases, only the emission from the $^5D_0$ level is observed, revealing that the high-energy host matrix phonons make the multi-phonon relaxation process predominant among the ^5D_J levels.

As we know, the parity intra 4f transition of the rare earth ions is forbidden in a symmetrical crystal field. However, if the crystal field is destroyed, the intra 4f transition of the rare earth ions is allowed, and its characteristic luminescence occurs. The transition of $^5D_0$ to $^7F_1$ is a magnetic dipole allowed, and its intensity shows very little variation with the bonding environment around Eu^{3+} ions. It is a dominant transition for the Eu^{3+} ions in an environment with an inversion symmetry. The transition of $^5D_0$ to $^7F_2$ is an electric dipole-allowed transition and is hypersensitive to the variation in the bonding environment of the Eu^{3+} ions. It becomes allowed when the bonding environment is distorted to non-inversion symmetries. As shown in Fig. 11, the emission intensity of the $^5D_0$-$^7F_1$ transition is much weaker than that of the $^5D_0$-$^7F_2$ transition which corresponds to a well-known behavior of the Eu^{3+} ions located in low symmetry sites [36]. From this point of view, the Eu^{3+} ions doped in the mesoporous silica thin films should be present in an environment with a low symmetry. In addition, the emission intensity of the Eu^{3+} ions-doped mesoporous silica thin films increases with increasing calcination temperature. It is well known that a lot of hydroxyl groups, residual adsorbed water, and organic groups exist in the mesoporous silica thin films fabricated by a sol–gel technique (as discussed earlier in the FTIR analysis). The presence of hydroxyl groups, residual adsorbed water, and organic groups can lower the luminescence efficiency of the Eu^{3+} ions through a non-radiative phonon quenching mechanism [37]. As discussed previously, the FTIR analysis reveals that with increasing calcination temperature, the content of hydroxyl groups, residual adsorbed water, and organic groups in the films decreases or disappears. Therefore, more efficient luminescence centers form in the films, which can increase the emission intensity.

In order to investigate the effect of dopant concentration on luminescence properties, the Eu^{3+} ions-doped mesoporous silica thin films with molar ratios of Eu/Si from 0.44 to 5.24% were calcined at 600°C for 4 h. Upon excitation of 246 nm, the transition from the excited $^5D_0$ level of the Eu^{3+} ions can be observed in the emission spectra of these films. As shown in Fig. 12, two main emission peaks of the Eu^{3+} ions-doped mesoporous silica thin films arise from the transitions of $^5D_0$-$^7F_1$ and $^5D_0$-$^7F_2$ [35]. As shown in the inset in Fig. 12, the integral emission intensity of the Eu^{3+} ions attributed to the $^5D_0$-$^7F_2$ transition centered at around 615 nm increases almost linearly with the Eu/Si molar ratio increasing up to 3.41%. With a further increase of the Eu^{3+} concentration from 3.41 to 5.24%, there is no obvious increase in the emission intensity. The high Eu^{3+} doping concentration would reduce the distance between the Eu^{3+} ions. As one pattern of the non-radiative relaxation process [38], the cross relaxation between the neighboring Eu^{3+} ions would take place and quench the luminescence efficiency with the Eu/Si molar ratio above 3.41% [39]. Practical fluorescence quenching due to the aggregation of Eu^{3+} is evident for Eu contents higher than 1% (molar ratio) in silica glass [20]. In our work, the fluorescence quenching concentration of 3.41% (Eu/Si molar ratio) in the Eu^{3+}-doped mesoporous silica thin films

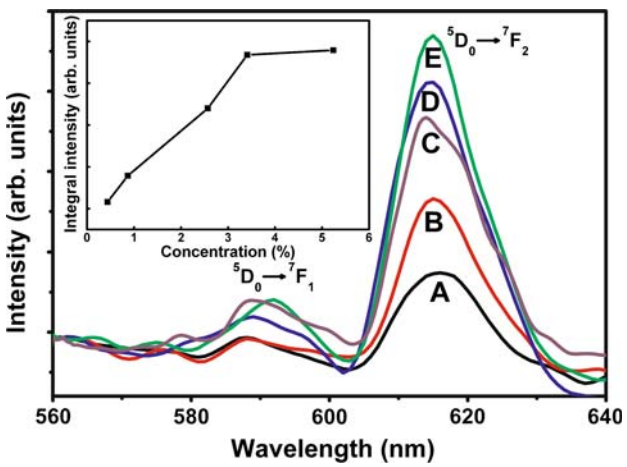

Fig. 12 The luminescence spectra of the Eu^{3+} ions-doped mesoporous silica thin films with an Eu/Si molar ratio of 0.44% (*curve A*), 0.87% (*curve B*), 2.57% (*curve C*), 3.41% (*curve D*), and 5.24% (*curve E*) calcined at 600°C for 4 h. The *inset* shows the dependence of the integral intensity of the 615-nm emission on the Eu^{3+} concentration

is higher than that of 1.2% in the Eu^{3+}-doped non-templated sol–gel silica in our comparison experiments. Ordered mesoporous silica thin films with large surface area can provide enough non-network oxygen species to coordinate and charge compensate the Eu^{3+} ions, which may enhance the overall solubility of Eu and prevent the aggregation of Eu^{3+} ions.

Conclusions

The ordered mesoporous silica thin films doped with the Eu^{3+} ions were prepared using non-ionic triblock copolymer surfactant as a structure-directing agent by sol–gel spin-coating and calcination process. The films with the thickness of about 205 nm are continuous, smooth, and dense without cracks and have ordered body-centered cubic structure of the *Im*3 *m* space group. Although the Eu^{3+} ion loading is up to an Eu/Si molar ratio of 5.24% and the calcination temperature is as high as 600°C, the body-centered cubic mesoporous structure of the films is well retained. The photoluminescence spectra show two main emission peaks attributed to the $^5D_0$-$^7F_1$ and $^5D_0$-$^7F_2$ transitions of the Eu^{3+} ions located in low symmetry sites. Furthermore, the intensity of the $^5D_0$-$^7F_2$ transition increases with increasing calcination temperature. The 615-nm emission intensity increases almost linearly with the Eu/Si molar ratio increasing from 0.44 to 3.41%.

Acknowledgments The work was supported by the International S&T Cooperation Program (ISCP) under 2008DFA50340, MOST, the Specialized Research Foundation for the Doctoral Programs (20070730022), MOE, China, and the National Natural Science Foundation of China (50872046).

References

1. C.T. Kresge, M.E. Leonowicz, W.J. Roth, J.C. Vartuli, J.S. Beck, Nature **359**, 710 (1992)
2. H. Yang, N. Coombs, I. Sokolov, G.A. Ozin, Nature **381**, 589 (1996)
3. C.J. Brinker, Y. Lu, A. Sellinger, H. Fan, Adv. Mater. **11**, 579 (1999)
4. B.J. Scott, G. Wirnsberger, G.D. Stucky, Chem. Mater. **13**, 3140 (2001)
5. W.C. Molenkamp, M. Watanabe, H. Miyata, S.H. Tolbert, J. Am. Chem. Soc. **126**, 4476 (2004)
6. A. Cabot, J. Arbiol, A. Cornet, J.R. Morante, F. Chen, M. Liu, Thin Solid Films **436**, 64 (2003)
7. S.-B. Jung, C.-K. Han, H.-H. Park, Appl. Surf. Sci. **244**, 47 (2005)
8. U. Ciesla, F. Schüth, Micropor. Mesopor. Mat. **27**, 131 (1999)
9. F. Gao, S.P. Naik, Y. Sasaki, T. Okubo, Thin Solid Films **495**, 68 (2006)
10. M.H. Bartl, B.J. Scott, H.C. Huang, G. Wirnsberger, A. Popitsch, B.F. Chmelka, G.D. Stucky, Chem. Commun. **2002**, 2474 (2002)
11. N.R.B. Coleman, N. O'Sullivan, K.M. Ryan, T.A. Crowley, M.A. Morris, T.R. Spalding, D.C. Steytler, J.D. Holmes, J. Am. Chem. Soc. **123**, 7010 (2001)
12. K.L. Frindell, J. Tang, J.H. Harreld, G.D. Stucky, Chem. Mater. **16**, 3523 (2004)
13. C.M. Leroy, T. Cardinal, V. Jubera, M. Treguer-Delapierre, J. Majimel, J.P. Manaud, R. Backov, C. Boissière, D. Grosso, C. Sanchez, B. Viana, F. Pellé, Chem. Phys. Chem. **9**, 2077 (2008)
14. K.L. Frindell, M.H. Bartl, M.R. Robinson, G.C. Bazan, A. Popitsch, G.D. Stucky, J. Solid State Chem. **172**, 81 (2003)
15. J.C. Yu, G. Li, X. Wang, X. Hu, C.W. Leunga, Z. Zhang, Chem. Commun. **2006**, 2717 (2006)
16. A.J. Silversmith, D.M. Boye, R.E. Anderman, K.S. Brewer, J. Lumin. **94–95**, 275 (2001)
17. V.C. Costa, M.J. Lochhead, K.L. Bray, Chem. Mater. **8**, 783 (1996)
18. J. Wang, H. Song, X. Kong, H. Peng, B. Sun, B. Chen, J. Zhang, W. Xu, J. Appl. Phys. **93**, 1482 (2003)
19. H. Yamane, Y. Kaminaga, S. Abe, T. Yamada, J. Solid State Chem. **181**, 2559 (2008)
20. W. Jia, H. Liu, S.P. Felofilov, R. Meltzer, J. Jiao, J. Alloys Compd. **311**, 11 (2000)
21. T. Yamada, H.-S. Zhou, H. Uchida, M. Tomita, Y. Ueno, T. Ichino, I. Honma, K. Asai, T. Katsube, Adv. Mater. **14**, 812 (2002)
22. P. Yang, D. Zhao, D.I. Margolese, B.F. Chmelka, G.D. Stucky, Chem. Mater. **11**, 2813 (1999)
23. P.C.A. Alberius, K.L. Frindell, R.C. Hayward, E.J. Kramer, G.D. Stucky, B.F. Chmelka, Chem. Mater. **14**, 3284 (2002)
24. J.H. Pan, S.Y. Chai, C. Lee, S.-E. Park, W.I. Lee, J. Phys. Chem. C **111**, 5582 (2007)
25. Q. Lu, Z. Wang, J. Li, P. Wang, X. Ye, Nanoscale Res. Lett. **4**, 646 (2009)
26. M.D. Alba, Z. Luan, J. Klinowski, J. Phys. Chem. **100**, 2178 (1996)
27. P. Innocenzi, P. Falcaro, D. Grosso, F. Babonneau, J. Phys. Chem. B **107**, 4711 (2003)
28. G. Duan, C. Zhang, A. Li, X. Yang, L. Lu, X. Wang, Nanoscale Res. Lett. **3**, 118 (2008)
29. J. Yin, L. Xiang, X. Zhao, Appl. Phys. Lett. **90**, 113112 (2007)
30. J. Wang, W.S. Brocklesby, J.R. Lincoln, J.E. Townsend, D.N. Payne, J. Non-Cryst. Solids **163**, 261 (1993)
31. W. Chen, R. Sammynaiken, Y. Huang, J. Appl. Phys. **88**, 1424 (2000)
32. L. Li, S. Zhang, J. Phys. Chem. B **110**, 21438 (2006)
33. M.F. Hazenkamp, A.M.H. van der Veen, N. Feiken, G. Blasse, J. Chem. Soc. Faraday Trans. **88**, 141 (1992)
34. C. Lin, H. Wang, D. Kong, M. Yu, X. Liu, Z. Wang, J. Lin, Eur. J. Inorg. Chem. **2006**, 3667 (2006)
35. N. Wan, J. Xu, T. Lin, X. Zhang, L. Xu, Appl. Phys. Lett. **92**, 201109 (2008)
36. M.A. Zaitoun, T. Kim, C.T. Lin, J. Phys. Chem. B **102**, 1122 (1998)
37. A.J. Berry, T.A. King, J. Phys. D **22**, 1419 (1989)
38. T. Ishizaka, R. Nozaki, Y. Kurokawa, J. Phys. Chem. Solids **63**, 613 (2002)
39. M. Yu, J. Lin, J. Fu, H.J. Zhang, Y.C. Han, J. Mater. Chem. **13**, 1413 (2003)